RHIC BACKGROUNDS AND THEIR EFFECT ON THE PHENIX MUON IDENTIFIER

Vince Cianciolo and Ken Read

Version 7/22/03

1. Description of the problem

The purpose of this technical note is to describe and characterize the effect of backgrounds due to the RHIC beam on the PHENIX Muon Identifier (MuID) and to discuss possible solutions. This note describes a variety of studies performed to reach these conclusions.

The MuID consists of two arms, located at the north and south ends of the PHENIX Experimental Hall. Each arm consists of five planes of Iarocci tubes (mounted inside aluminum panels) interleaved with steel absorber plates of 10 and 20 cm thickness. The layers of Iarocci tubes are called "gaps", and they are numbered from 0 to 4, with gap-0 being closest to the interaction point and gap-4 is closest to incoming-beam background sources.

Beam-related backgrounds cause two distinct problems for the MuID. First, they increase the false-hypothesis trigger rate. In fact, the MuID trigger rates greatly exceed the minimum bias interaction trigger rate (!), and they have reached levels which are unacceptable due to PHENIX bandwidth requirements. As a consequence we are forced to require a coincidence of the MuID trigger with the minimum bias trigger. This results in a loss in acceptance (given a decent vertex offline from the PHENIX MVD) since 25% events in which a J/Ψ is created do not fire the interaction trigger (BBC). Also, we are unable to make a systematic check of the MuID trigger efficiency (looking at unconditioned MuID triggers for BBC-scaled trigger events). Finally, even with the minimum bias trigger in coincidence, our trigger is dominated with accidental coincidences and we are forced to scale down and/or lose acceptance with more selective triggers (e.g., one that requires both J/Ψ daughter muons to penetrate to the deepest gap.)

The second problem that beam-related backgrounds cause for the MuID is an increase in the current drawn by the Iarocci tubes simply due to the significantly larger number of particles passing through them. Such current draw (and associated extremely high hit rates) can cause premature aging of the tubes. We do not yet have conclusive evidence of aging and we intend to study this possibility (and gas-mixture options for mitigating such a problem) with studies over the next few months. We are considering implementing a bubbler that will be capable of introducing trace amounts of isopropanol and/or water, which has been shown to eliminate and even reverse aging in similar detectors with similar operating gas [1]. Even if aging concerns turn out to be baseless, the higher currents render the data very difficult to analyze. To understand this, consider the in-panel high voltage distribution, shown in Figure 1. Since the panels are completely unserviceable for the expected lifetime of PHENIX (more than ten years), the high-voltage supply for each Iarocci tube is protected with a 400 M-Ohm current-limiting resistor. The purpose of this resistor is to allow a high-voltage supply (which services ~25 Iarocci tubes) to continue to function even if as many as four tubes in the chain have broken wires. This is discussed in some more detail in Table 1 (below). The consequence of this resistor, in the face of unexpected hit-rates (and therefore current draw), is that the effective voltage on the tubes is lowered. For 10 μA current draw for an HV chain (regularly seen during Run-2) each tube draws ~0.5 μA, for an effective voltage loss of 200V. From Figure 2, which shows the MuID efficiency versus high voltage, it can be seen that such a drop in effective voltage causes a significant efficiency loss. Since the currents in the panels can change significantly over the course of the run (as beams are steered and/or collimated) this results in an unacceptable time-dependent efficiency variation that can render the data useless.

Throughout the run, especially at the beginning of fills, the MuID suffered from high current draw and high trigger rates. This issue was so severe during Run 3 that the detector was systematically forced to be turned off during the beginning of most fills and therefore miss much of the highest luminosity conditions.

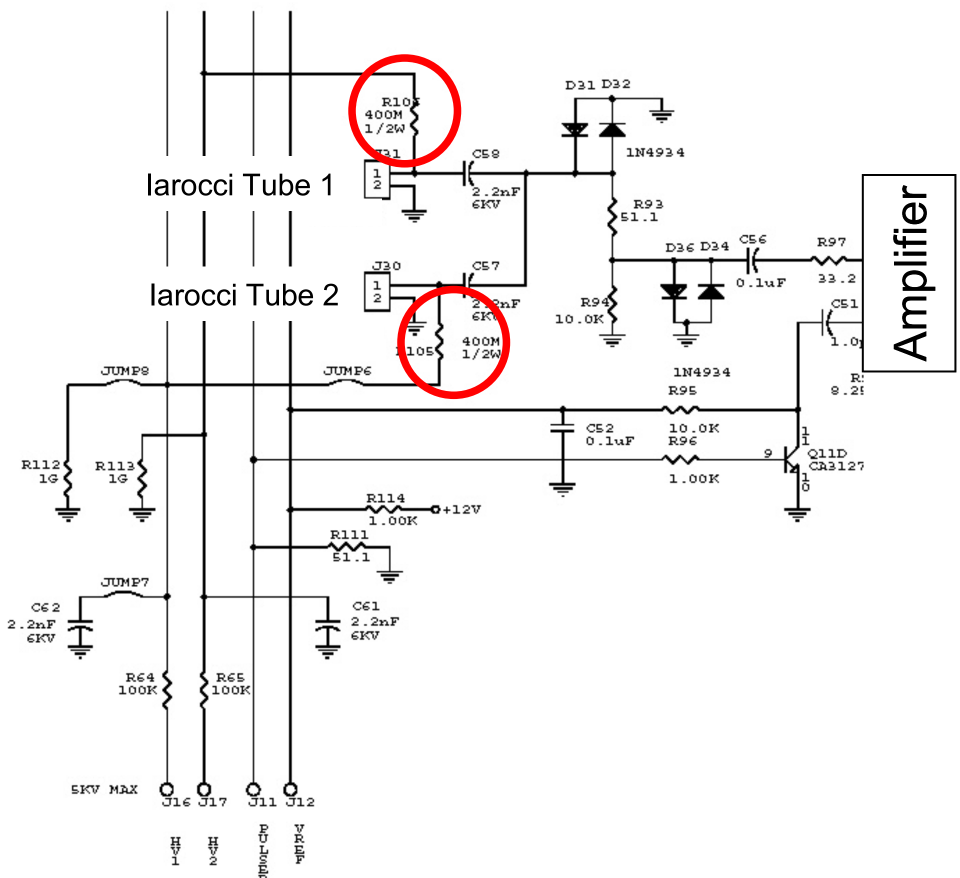

Figure 1. Schematic diagram showing high voltage distribution and preamplifier for the Iarocci tubes. The 400 M-Ohm current limiting resistors are circled.

Probability for a chain to be enabled (assume 1% failure rate per year)

Year	Maximum number of broken wires: 0	1	2	3	4
1	0.82	0.98	1.00	1.00	1.00
2	0.67	0.94	0.99	1.00	1.00
3	0.54	0.88	0.98	1.00	1.00
4	0.44	0.81	0.96	0.99	1.00
5	0.36	0.74	0.92	0.98	1.00
6	0.29	0.66	0.89	0.97	0.99
7	0.23	0.59	0.84	0.95	0.99
8	0.19	0.52	0.79	0.93	0.98
9	0.15	0.45	0.73	0.90	0.97
10	0.12	0.39	0.68	0.87	0.96

Rlimit (Giga-Ohm) is given by Nmax/(Imax / Vop - 1), where:

Rlimit is the value of the current limiting resistor,
Nmax is the maximum number of broken wires that an HV supply can maintain,
Imax is the HV supply maximum current (uA) out of the HV supply,
Vop is the operating voltage (kV),
And the -1 is from the 1 Giga-ohm bleeder resistor.

Want to be able to maintain 95% efficiency after 10-years, so we need to allow for 4 broken wires. With our data at the time of panel construction (Vop = 5.000 kV, Imax = 100 uA), Rlimit was 250 M-Ohm and we went with 400 M-Ohm to allow some margin of error on the supply current.

With current data (tube mortality better than 1%/year, Vop = 4.300 kV, Imax=200 uA) we could have used 75-100 M-Ohm, which would have mitigated the problem somewhat, but the resistors can't be changed.

Table 1. Probability for an entire HV chain to be disabled due do excessive current draw given the maximum allowable number of broken wires (a function of operating parameters and the current-limiting resistor value) and the year of the experiment. Accompanying text details the choice of the resistor value (400 M-Ohm).

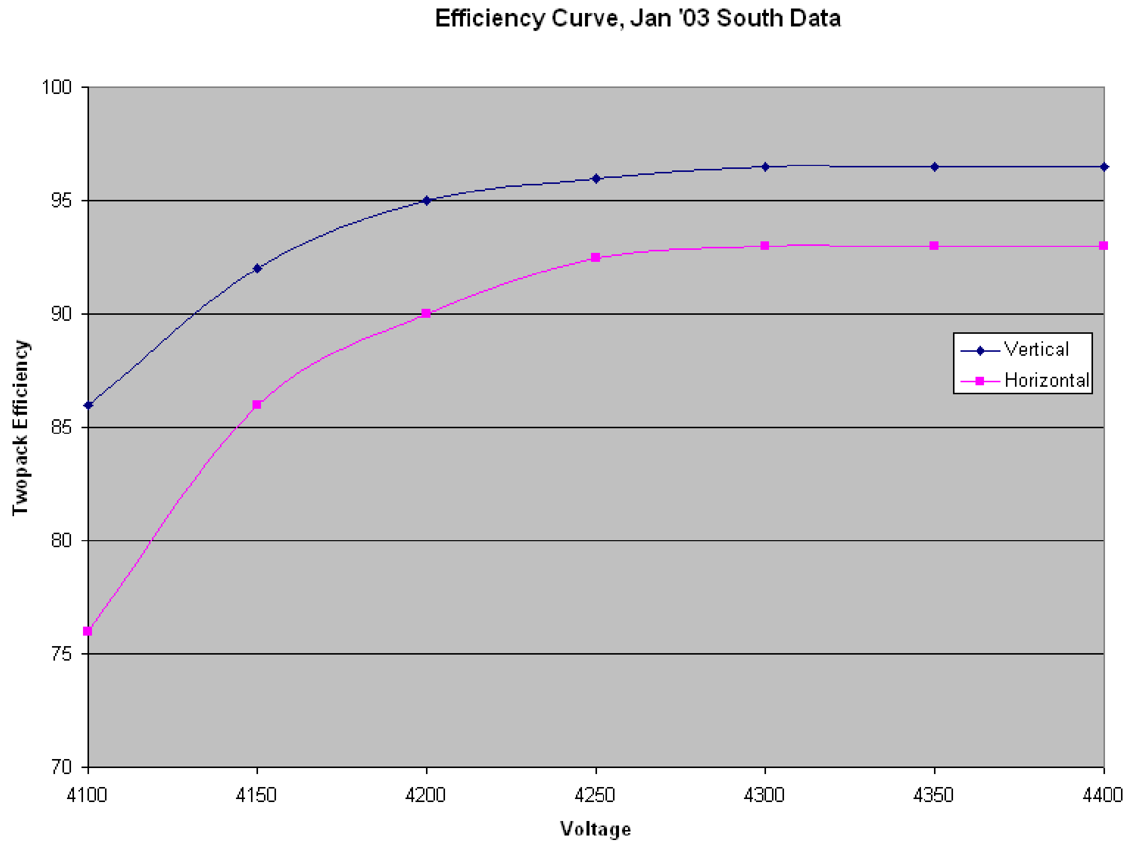

Figure 2. Iarocci tube efficiency as a function of high voltage. Normal operational voltage is currently 4300V. Most chains can be raised to 4400V or more once an automatic-reset feature is in place in the HV control program. Improved beam backgrounds also would help here since without these backgrounds the chains are much less likely to trip at higher voltages.

2. Mechanisms to examine the problem

We have explored a variety of approaches to study this problem. These are described in this section.

MuID Current Monitors

We kept a continuous log of the currents on the different MuID HV supplies. Figure 3 shows a graphical snapshot of the MuID HV current monitor when backgrounds were particularly bad. Upper (lower) panels are above (below) the thick black line. Consecutive pairs of columns are labeled GP0_H, GP0_V, etc. and refer to Gap-0 Horizontal chains, Gap-0 Vertical chains, etc.

Correlating changes in these distributions versus beam conditions proved to be somewhat difficult for a variety of reasons. Beam conditions changed significantly due to intensity, steering, and collimation. Also, some chains have tripped (circled in red) and some chains have individual tubes with high current draw (circled in black). Nevertheless, one can make the following observations:

- Upper panels have worse current draw than lower panels. The black rectangles surround chains which are mirror images of each other through a horizontal plane at beam height.
- Current draw increases with depth. This is shown by the chains surrounded by blue and purple rectangles. These rectangles surround groups of tubes at the same position transverse to the beam, but increasing to the right in proximity to the RHIC tunnel.
- Horizontal/Vertical tube current trends (red arrows) are different for upper and lower panels. For upper-panel vertical tubes and lower-panel horizontal tubes the current decreases monotonically with distance from the beam. On the other hand, for lower-panel vertical tubes and upper-panel horizontal tubes the maximum is somewhat displaced from beam. For the lower-panel vertical tubes this is almost certainly due to shielding by the concrete mezzanine on which the beamline is mounted. For the upper-panel horizontal tubes this is likely to be a result of the test shielding we installed during the run.

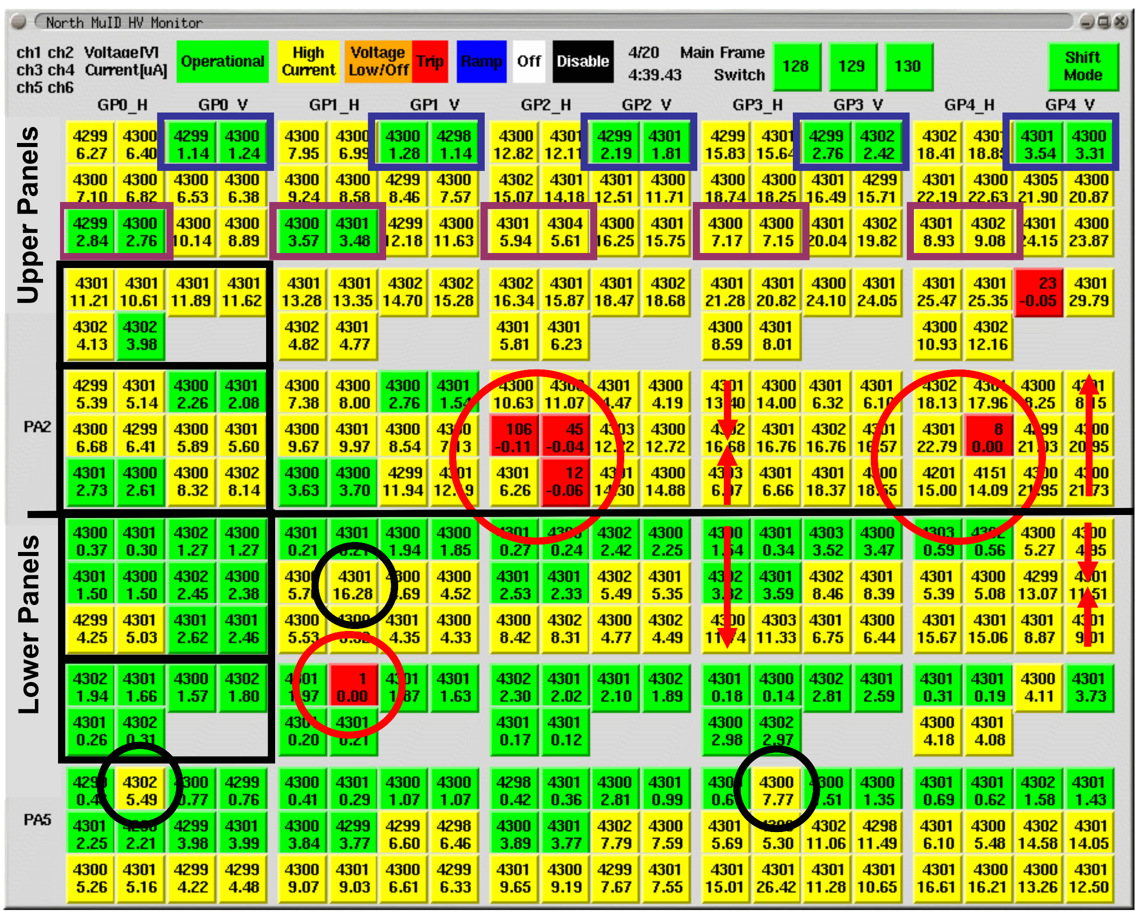

Figure 3. Muon identifier HV currents shown as the lower number in each colored box. The upper value is the voltage. Symbols are described in text.

We were also able to use the current monitor to show the correlation between the current draw and the number of hits in the Iarocci tubes. To do this we collected data in a special "clock trigger" run. By using forced-accept triggers on random beam clock signals (the 106 RHIC bunch-crossing clock), we effectively opened up a gate in the data acquisition system for a fixed amount of time. We then counted the number of hits and normalized to the gate length. Figure 4 shows the results of this run for the North Arm vertical tubes in the upper-west panels across all gaps. These panels had the largest backgrounds and were the cleanest in terms of tripped HV chains. The *y*-axis is the rate per tube in kilohertz, the *x*-axis is the observed current draw. The line is a straight line fit to the data. There are several things to note about this plot:

- The backgrounds for this particular run were especially bad. For the most part the currents were negligible in gap-0.
- The currents increase with gap depth (since the downstream gaps are less shielded by the MUID absorber plates from particles entering from the rear of the detector.
- When the detector efficiency (lowered to the excessive current draw) is used to correct the observed rates it is seen that the gap-4 rates are in excess of 250 kHz (!) per tube.
- To put this hit rate into perspective, the average MuID hit rate for minimum bias pp collisions is 1 hit/arm/event, and this has a significant contribution from background hits. If we make the worst-case assumption that this rate is entirely due to collisions, then at the highest luminosity expected (20 MHz minimum bias pp collisions), the expected hit rate from collisions would be an average rate of 7 kHz/tube, which should cause negligible current draw and related inefficiencies. The AuAu hit rates at 40 times design luminosity are similar.

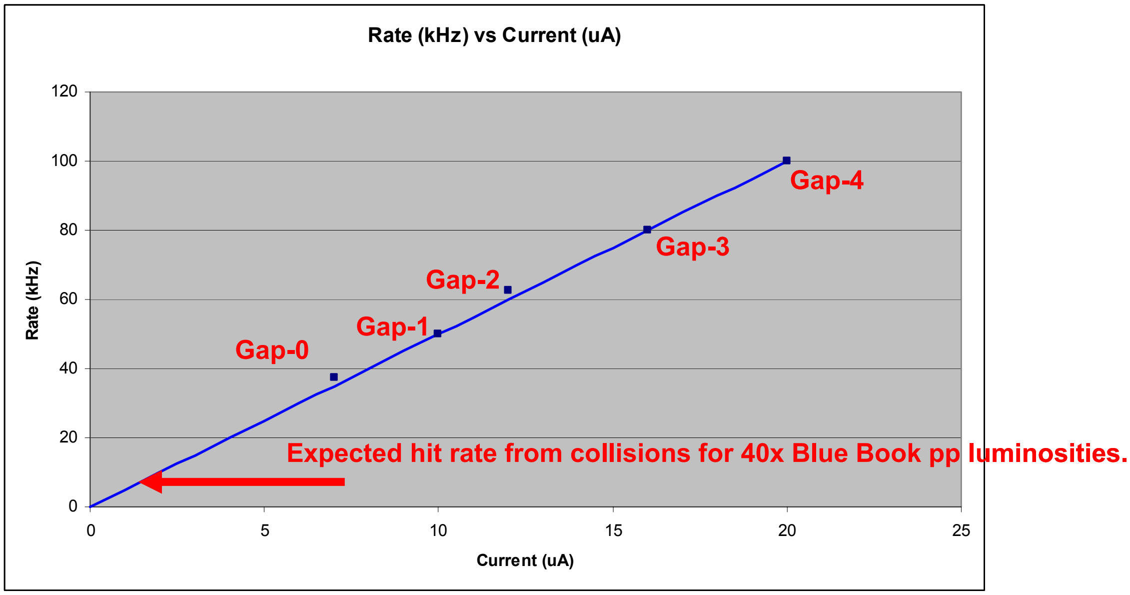

Figure 4. Results of a special "clock trigger" run. See text for description.

Scintillator Paddles

Although measuring the currents in the MuID HV supplies is of course the most direct measure of the problem, this approach suffers from the fact that it can provide no information at the very beginning of a store, when we did not feel it was safe to turn the HV on. To get around this limitation, we installed six scintillator paddles and sent their scaler rates to MCR. Three scintillator paddles were installed at three locations in the RHIC tunnel south of PHENIX (S1 – S3), as shown in Figure 5, below. Three additional scintillators were installed in mirror locations in the tunnel north of PHENIX.

The hit rates in the scintillators varied by orders of magnitude depending on beam conditions. In general, high hit rates correspond to more background particles striking the MuID, greater MuID hit rates, and higher MuID HV current draw. The correlation between scintillator hit rate and MuID current draw was not perfect. This is not particularly surprising given the fact that the acceptance of the MuID and the scintillator paddles was quite different. Also, this acceptance difference depends strongly on the source of the backgrounds, which in turn depends on beam conditions such as steering, collimation and species. However, the correspondence was good enough that we learned how low the scintillators rates needed to be for it to be safe to turn the chambers on and start a "muon-in" run. The correspondence was also good enough to allow MCR to use them as a tool to aid in steering and collimating the beam to optimize running conditions.

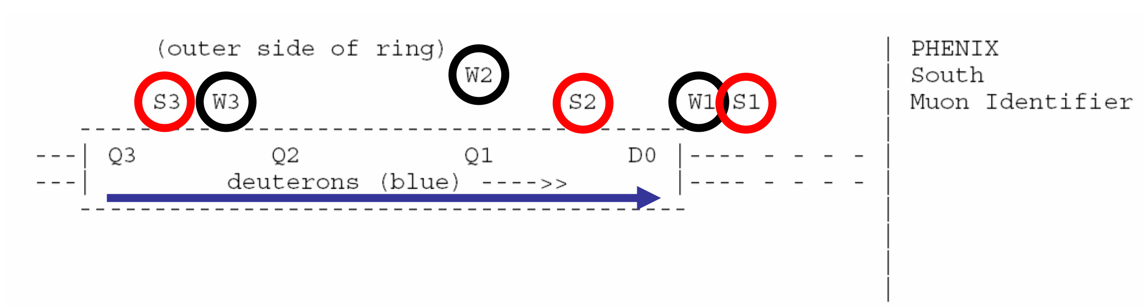

Figure 5. This figure shows the locations of scintillator paddles (S1, S2, and S3) and test shielding walls (W1, W2, and W3) in the RHIC tunnel south of PHENIX. Three additional scintillator paddles and shield walls were installed in mirror locations in the tunnel North of PHENIX.

Test Shielding

Trial shielding stations (W1-3 in Figure 5) each consisting of 2 feet of iron-loaded concrete (~2.5 Λ_I) were placed in the tunnel next to the beam line. We were unable to perform systematic studies in which shielding parameters (e.g., positions, thickness, composition) were changed under identical beam conditions. As a result it is difficult to quantify the effects of the shielding. However, the qualitative observation was that the shielding distributed the currents in gap-4 and greatly reduced the currents in gap-3. This is consistent with a picture in which the shielding intercepts high-energy particles, reduces their flux and energy somewhat, and spreads them out in angle. A 2.5 Λ_I shield is not nearly thick enough to stop particles approaching 100 GeV. They will deposit much of their energy in the shield, but not all of it, so that the shield itself acts as a lower-energy, larger-emmittance source of background.

Source Imaging

We attempted to "image" any source of background in the tunnel striking the MuID from the back. We did this by collecting some data without the requirement of a coincidence with the minimum bias trigger and then reconstructing that data without a requirement that MuID roads project to the PHENIX vertex. Although we did reconstruct MuID roads that clearly projected to locations in the RHIC tunnel we did not observe any point-like source. Rather, it appeared that there was essentially a line source extending over a large range in z. It should be noted however, that the pointing resolution of the MUID alone, especially for low-angle tracks is quite poor, and obscures our ability to see a point source.

3. Limiting fragmentation

Backgrounds coming from the tunnel upstream of the MuID must have relatively shallow angles (large pseudo-rapidity) in order to make it into the MuID. BRAHMS data, shown in Figure 6 [], beautifully illustrates the relevance of the concept of "limiting fragmentation" to high-rapidity particle production, and to the understanding of the tunnel backgrounds. From the BRAHMS data (main figure) we see that particle production for $\eta > 3$ is independent of centrality. By scaling to the beam frame ($\eta' = \eta - y$) and scaling by the number of projectile participants ($N_{part}/2$ in this symmetric case) we see agreement with CERN fixed-target heavy ion collisions. This scaling holds over a large range of collision energy and species. This is intuitively understandable because any particle near the beam-frame must have undergone (or been produced by) only "soft" collisions. The RHIC beam pipe has a radius $r = 6.35$cm. Since beam-scrape (or beam-gas) necessarily occur inside the beam pipe, particles will travel for some distance before exiting the beam pipe. It turns out that at RHIC energies this distance can be significant, as indicated by the numbers immediately above the x-axis which show how far particles at different η will travel before striking the beam pipe.

So far this discussion has focused on produced particles. For heavy ion projectiles there will also be spectator nucleons that have even higher pseudo-rapidity and which therefore travel even farther before exiting the beam pipe. This is illustrated in Figure 7, which shows the spectator distribution as a function of pseudo-rapidity measured at CERN []. The pseudo-rapidity is nicely given by expectation that spectators have Fermi momentum (~200 MeV) in the transverse direction, and p_{beam} in the direction of the beam. For RHIC energies, this says that spectators will hit the beam pipe 31 meters from their collision point. Not that this implies that there will be a species dependence in the background, even if scraping locations and the beam-gas/beam-scrape ratio were identical – heavy ion beams will lead to backgrounds that are more distributed around the ring.

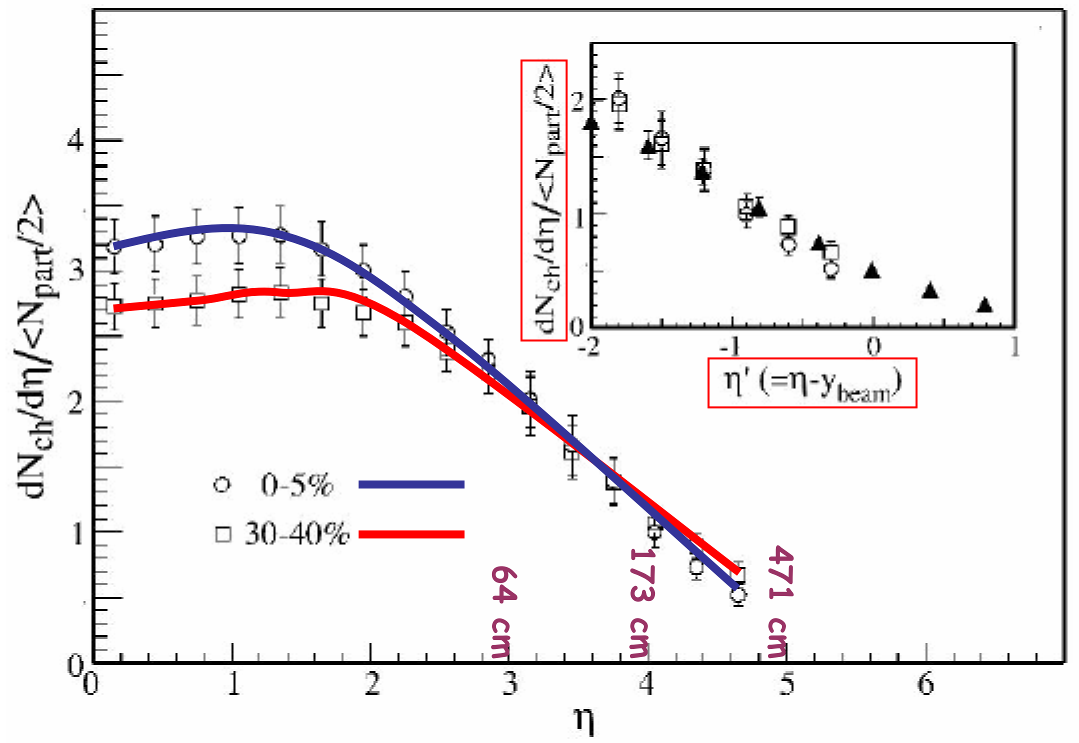

Figure 6. This figure illustrates the concept of limiting fragmentation by showing N_{part} scaling of high-rapidity charged particle multiplicities $\sqrt{s_{NN}}$ = 130 GeV/nucleon collisions in BRAHMS []. Central collisions are shown in blue and mid-central are shown in red. The inset shows that this scaling holds from CERN to RHIC energies if scaled to the projectile reference frame.

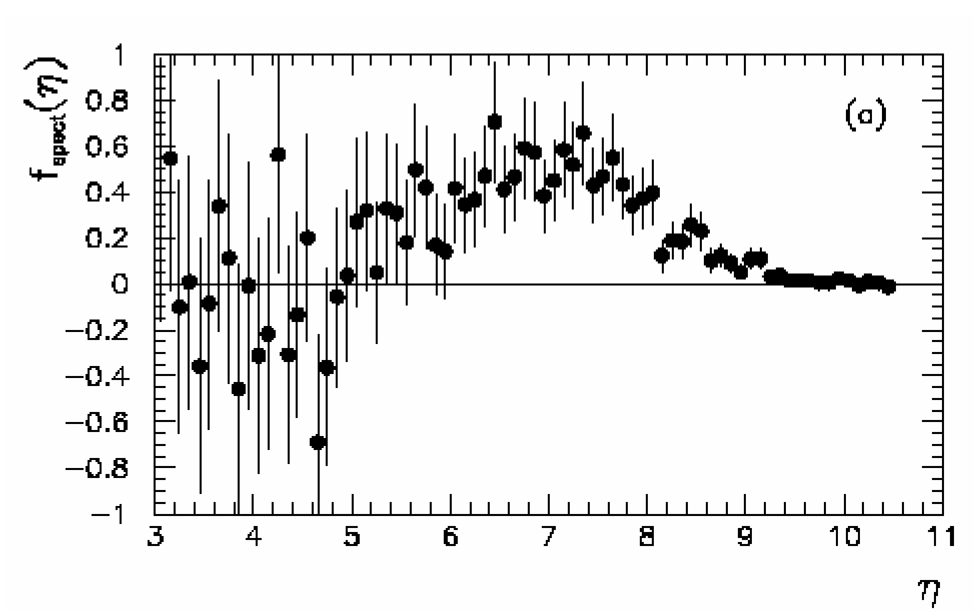

Figure 7. Spectator distribution as a function of pseudorapadity [].

These high pseudo-rapidity particles will exit the beam pipe at very glancing angles, thus going through many cm's of stainless steel in the beam pipe despite the 2mm pipe wall thickness. This is ~ $1\Lambda_I$, so that the beam pipe acts as a nearly perfect hadron amplifier. In addition, the shower locations along the length of the beam pipe will be new background sources, turning large sections downstream of any beam interactions into a line source.

4. Identifying the problem

The problem is not beam-beam collisions

The best evidence that the primary source of background is not beam-beam collisions is the fact that the scintillator rates and currents could be extremely high even with only one beam in the machine (true for the arm directly exposed to the incoming beam: South arm / blue beam; North arm / yellow beam). A supporting piece of evidence is the fact that the MuID trigger rate was far higher than the minimum bias trigger rate (instead of the expected 500 times less). This indicated that there was activity in the detector sufficient to fire a very restrictive trigger when there wasn't a collision inside our event vertex.

The problem is not (primarily) beam-gas collisions

The best evidence for this is the fact that the scintillator rates were quite small prior to collisions but after the beam had been brought up to full energy. Furthermore, the backgrounds could be reduced by orders of magnitude when the beams were steered and/or collimated. Such activity would have no effect on beam-gas backgrounds.

This does not mean that there is no beam-gas background. Such a component, which from an accelerator perspective can only be mitigated through vacuum improvements, may exist. It was not the primary source of the overwhelming backgrounds at the beginning of the store, but it could be a significant component of the backgrounds that remained after steering and collimation - both these types of backgrounds will look identical to us. It is important to note that if there is such a component it will only get worse as beam intensities go up. But it is also true that shielding that is effective against beam-scrape backgrounds (due to their extent along the beam) will also be effective against beam-gas backgrounds. If problems persist even after shielding, careful steering/collimation systematic studies can be done to determine if there is a beam-gas component that needs to also be reduced.

The problem is (primarily) beam-scrape collisions

In addition to the points used above to eliminate beam-beam collisions and beam-gas collisions as major components of the background, we have direct evidence that the MuID is very sensitive to beam-scrape by-products: the insertion of the polarizer targets more than ½-way around the ring increases trigger rates by orders of magnitude. This proves that we are sensitive to beam scrape even if the source is very far away.

There is also evidence that scraping of the beam is occurring inside the quad triplets immediately upstream of the interaction point where beam focusing occurs. Studies by MCR indicate that if the beams are scraping, the quad triplets are a likely site to suspect since the beam size is large there. BRAHMS has studied backgrounds using dosimeters and found evidence that the background particles come from the quad triplets. We have been able to study this with the tunnel scintillator paddles. Figure 8 shows the scintillator rates as a function of time after the beams were dumped. The scintillators see a two-component activation of nearby material. The longer (150 sec half-life) component is due to the decay of a meta-stable state of ^{53}Fe. It is interesting to note that this activation was only seen for Au beams.

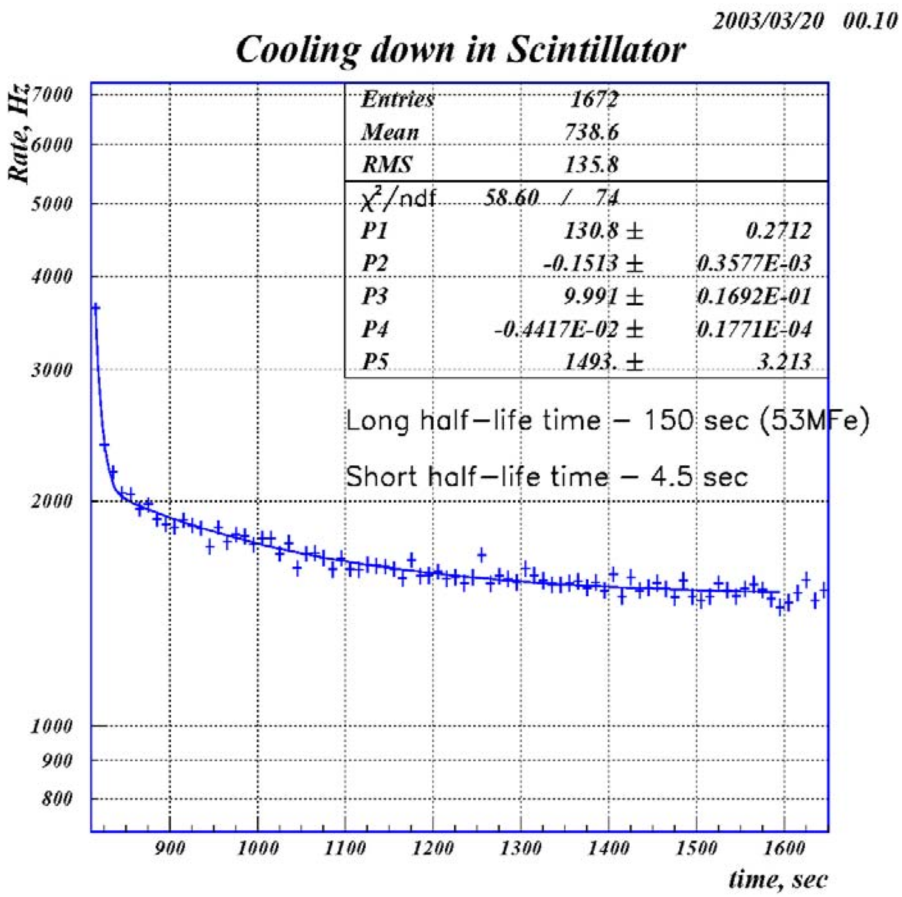

Figure 8. Scintillator rate due to beam related background as a function of time after dumping the beam. The characteristic time constant indicates activation of ^{53}Fe.

5. Solving the problem

We simply cannot afford to not solve this problem, at least to a significant extent, this summer. Run-4 will likely be the last long AuAu run for some time to come, and it is critical for the PHENIX J/Ψ measurement program to have the MuID operational, with stable efficiencies, acceptable trigger rates, and no worries about chamber aging.

There are few options for mitigating the problem. The only mechanism under PHENIX control to reduce panel currents is to turn off the detector. There are no acceptable options for reducing the inefficiencies caused by these currents: 1) The current-limiting resistors cannot be replaced with a smaller resistor value. They are inaccessible. 2) The efficiency plateau could be widened by running the Iarocci tubes in streamer mode (as opposed to proportional mode) but this would greatly exacerbate aging concerns. And, in this mode each hit draws significantly more current, so that the voltage drop across the current-limiting resistor is larger, canceling out the wider efficiency plateau. We do have some ability to reduce our trigger sensitivity to the backgrounds. We will have a LVL1 trigger this year capable of tracking muon candidates and requiring that they come from the vertex. This will still provide insufficient event selectivity at the highest luminosities without resorting to a trigger that has significant acceptance loss.

There are some mechanisms under machine control that can be used to reduce backgrounds. Optimized steering and an aggressive collimation regime have been shown to reduce backgrounds significantly. However, these techniques do not guard against a beam-gas component to the backgrounds. It is also not clear that these techniques will be sufficient as the machine intensities go up, and furthermore it takes some non-negligible time to implement these mechanisms. The consequences of this delay between the start of a store and the time at which the MuID can take valid data has severe consequences for the total integrated luminosities, especially for Au beams with their relatively short life time. This is illustrated in Figure 9, below.

This leaves the option of shielding, which will be required to: 1) guard against increased backgrounds due to increases in beam intensity, 2) guard against a possible beam-gas component to the background that cannot be cleaned up via steering or collimation, 3) minimize delay between the start of a store and the time at which we can collect valid data.

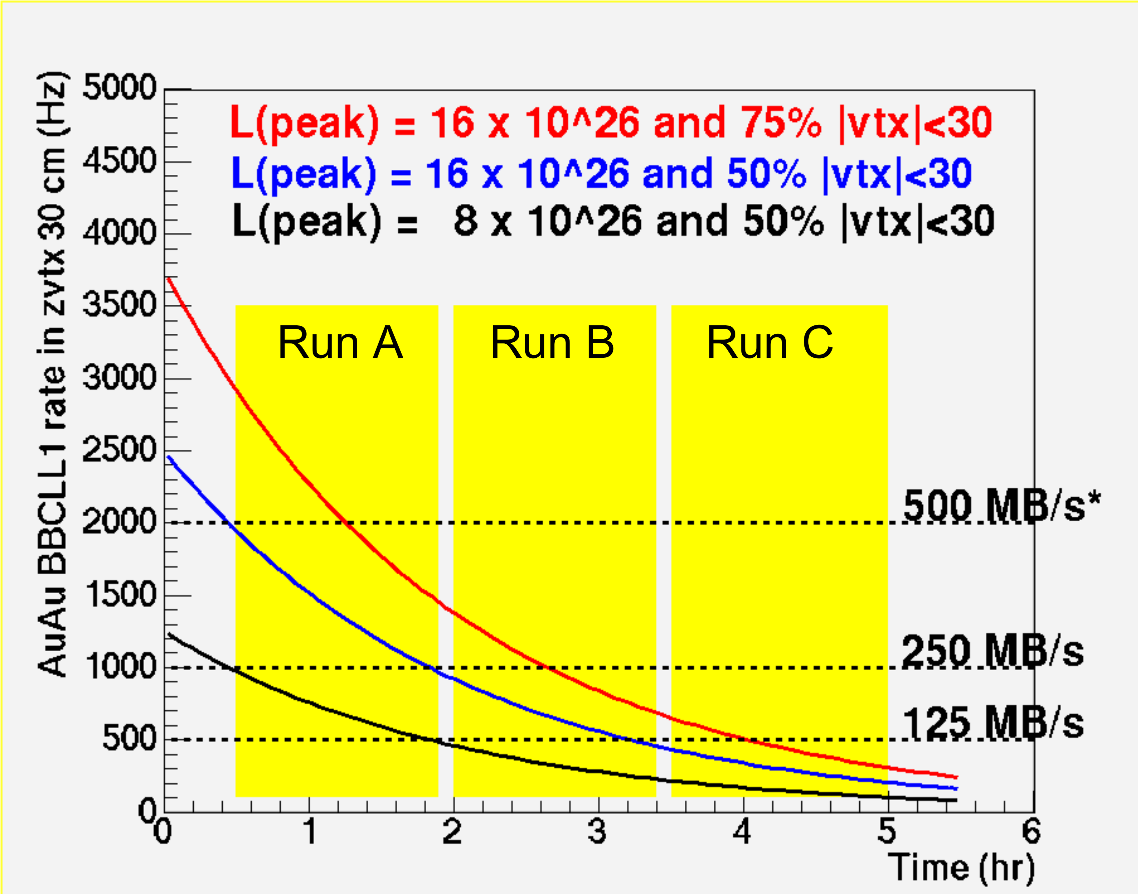

Figure 9. This plot [] shows three possible scenarios for PHENIX data collection in Run-4. The three colored exponential curves assume different peak luminosities and different fractions of events within our vertex cut (30 cm). The half-life is assumed to be two hours. The dashed lines indicate three different possibilities for the maximum archiving rate. The expectation is that all events which satisfy a selective LVL2 trigger will be recorded with the bandwidth for minimum bias collisions adjusted during each run to fill the available bandwidth. This means that more than half of all LVL2-triggerable data (which includes $J/\Psi \rightarrow \mu\mu$) will is available in the first one-hour run and will be lost if there is even a one hour delay in getting to beam conditions (steering/collimation) clean enough for MuID operation.

6. Shielding studies

Kin Yip from CAD has performed some simulations to study the backgrounds and possible shielding solutions. He also went to Fermilab for discussions with N. Mokhov and D0 physicists who have recently completed a very successful shielding project.

Thus far, the simulations have been performed using MCNPX (newest version 2.5.c) with 100 GeV protons as the source scraping the inner radii of Q2/Q3 magnets. MCNPX does not simulate the magnetic fields, which may be important for a quantitative examination of the problem. He is now trying to use MARS (written by N. Mokhov) which does simulate the magnetic fields. Also, only protons/neutrons are turned on at the moment. Figure 10 shows background flux at the MuID according to this simulation (before shielding).

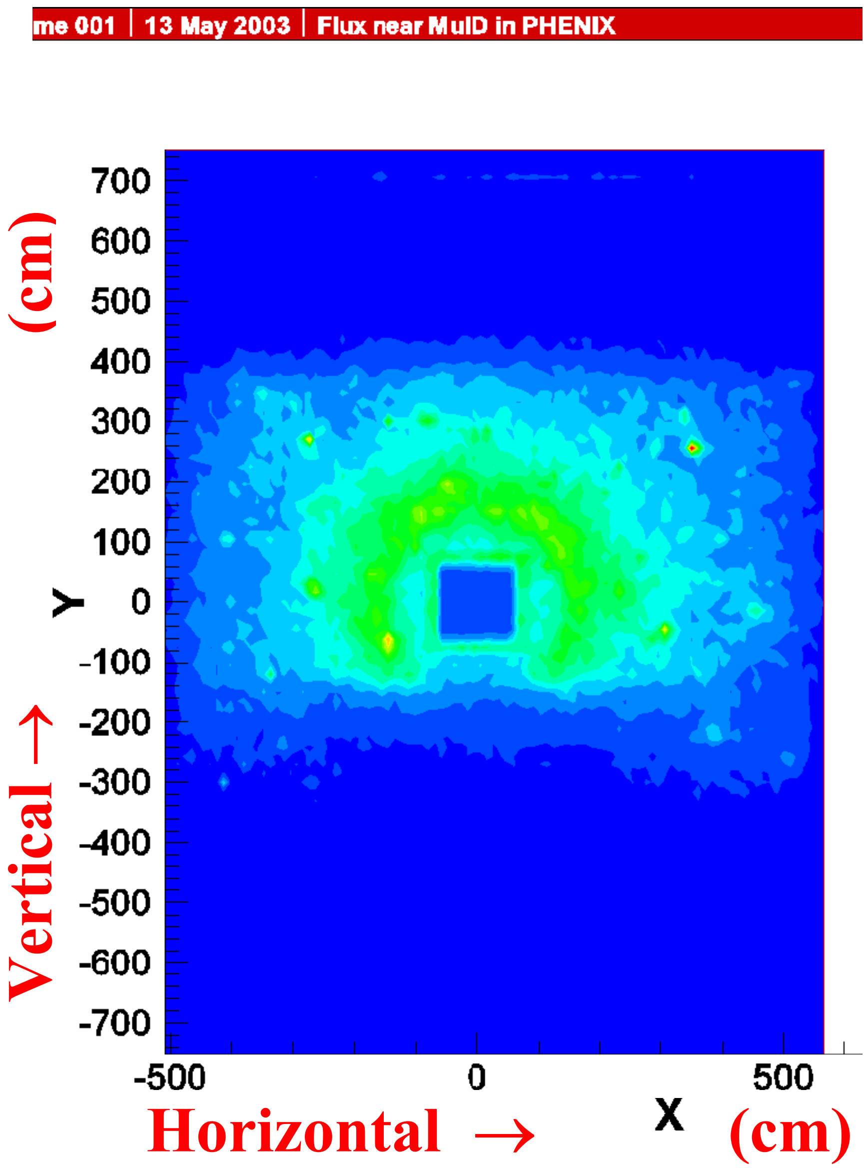

Figure 10. This figure shows the simulated distribution of particles striking the back of the PHENIX MuID without any shielding. (Courtesy of Kin Yip, RHIC.) The beam enters the MuID at $x=y=0$. The blue square in the center is not instrumented. The vertical asymmetry of the distributions is due to the concrete mezzanine on which the beam line is mounted.

Despite these limitations, these simulations have been very useful in understanding the nature of the problem and developing a strategy to mitigate the problem. Several shielding locations, configurations, and compositions were tried and some general conclusions can be drawn:

- It was observed that even when the beam-scrape interactions in the simulation occurred at Q3 (the quadrupole magnet furthest upstream), shielding was much more effective when it was closer to the MuID. This was the first clue that particles entering the MuID travel inside the beam pipe and cryostats for many meters before they are sufficiently far (in the transverse direction) from the beam to be intercepted by possible shielding.
- Since the particles are high-energy, many interaction lengths are needed to stop them. This argues for iron shielding as opposed to concrete shielding.
- It is very important to use the complex formula of realistic steel (rather than simply ^{56}Fe) in the simulations as suggested by Y. Efremenko (Univ. Tennessee), and confirmed by N. Mokhov (FNAL). Real steel does a much better job of stopping slow neutrons than ^{56}Fe. So, the benefits of steel are much clearer when this is taken into account.

The effectiveness of different compositions and locations of five-foot thick shielding walls against protons and neutrons are shown (as a function of particle energy when it hits the MuID) in Figures 11 and 12. Fluxes are reduced by roughly two orders of magnitude across the entire spectrum.

It is much more difficult to erect a real steel wall than to erect one in a simulation. In particular, in order to shield the outer reaches of the MuID with a wall near the DX magnet would require an enormous wall extending over the lip of the mezzanine. This is too much steel, is too difficult to support and restricts access unacceptably. One possible solution is to erect three walls at different z-locations, each of which, in effect, shields a different portion of the beamline. Such a configuration is shown in Figure 13, in a plan view of the South tunnel. Such a configuration also has issues because it will require a large amount of steel that will be difficult to install and which will require work-arounds in order to maintain access.

This configuration still needs to be simulated, but it does a good job of blocking the entire MuID from the entire beamline, as shown in Figure 14.

7. Summary

The MuID suffers from non-collision related backgrounds due to excessive hit rates which can cause pre-mature aging, reduced efficiency, and excessive trigger rates. This background is different from the collision-related backgrounds that were successfully addressed last year via the square-hole shielding and the south MuID collar. Collimation and steering can reduce backgrounds during a run, but any delay between the start of a store and reduction of backgrounds to acceptable levels has a dramatic effect on the total integrated luminosity that the muon arms can process due to the two-hour luminosity half-life. The only way to thoroughly address this problem is through massive shielding in the RHIC tunnels to block the MuID from line-of-sight of the beam. The exact location of the background source is extremely difficult to pin down, but due to limiting fragmentation is likely to be extended over many meters. Therefore the shielding should cover the entire beamline to the extent practical.

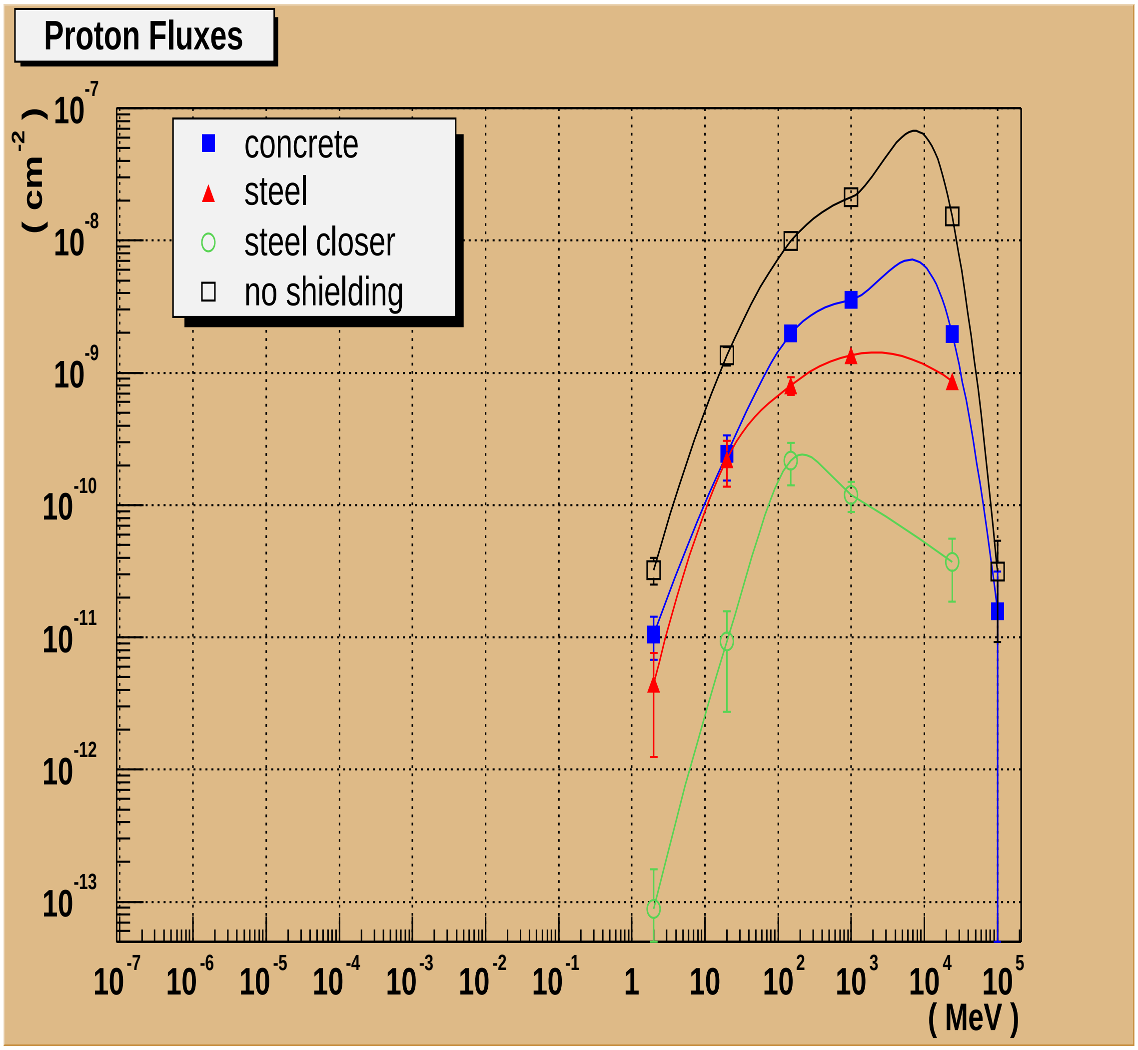

Figure 11. This figure shows the simulated proton energy spectrum due to beam-related backgrounds at the back of the MuID versus neutron energy. The flux is reduced by simulated shielding composed of concrete (blue), steel (red), or steel positioned very close to the MuID (green). (Courtesy of Kin Yip, RHIC.)

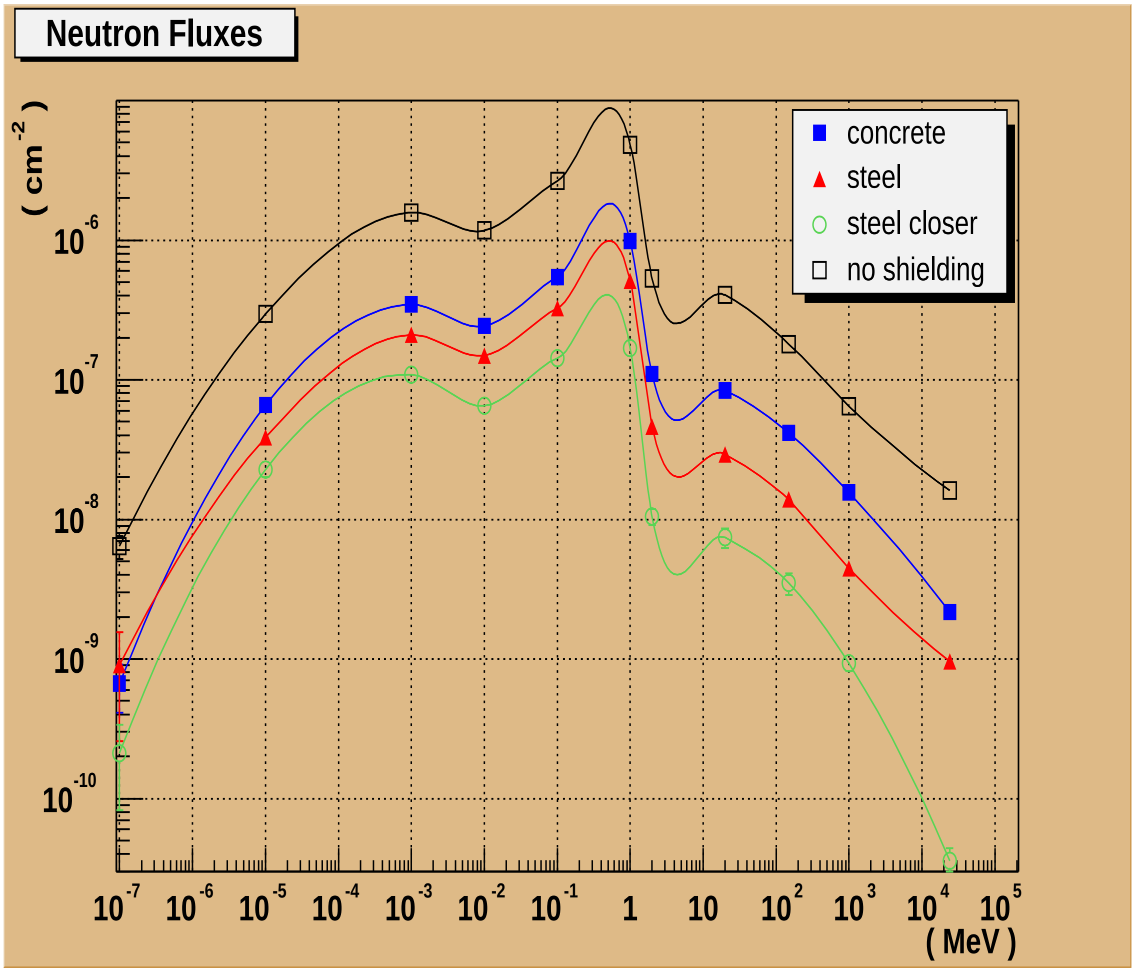

Figure 12. This figure shows the simulated neutron flux due to beam-related backgrounds at the back of the MuID versus neutron energy. The flux is reduced by simulated shielding composed of concrete (blue), steel (red), or steel positioned very close to the MuID (green). (Courtesy of Kin Yip, RHIC.)

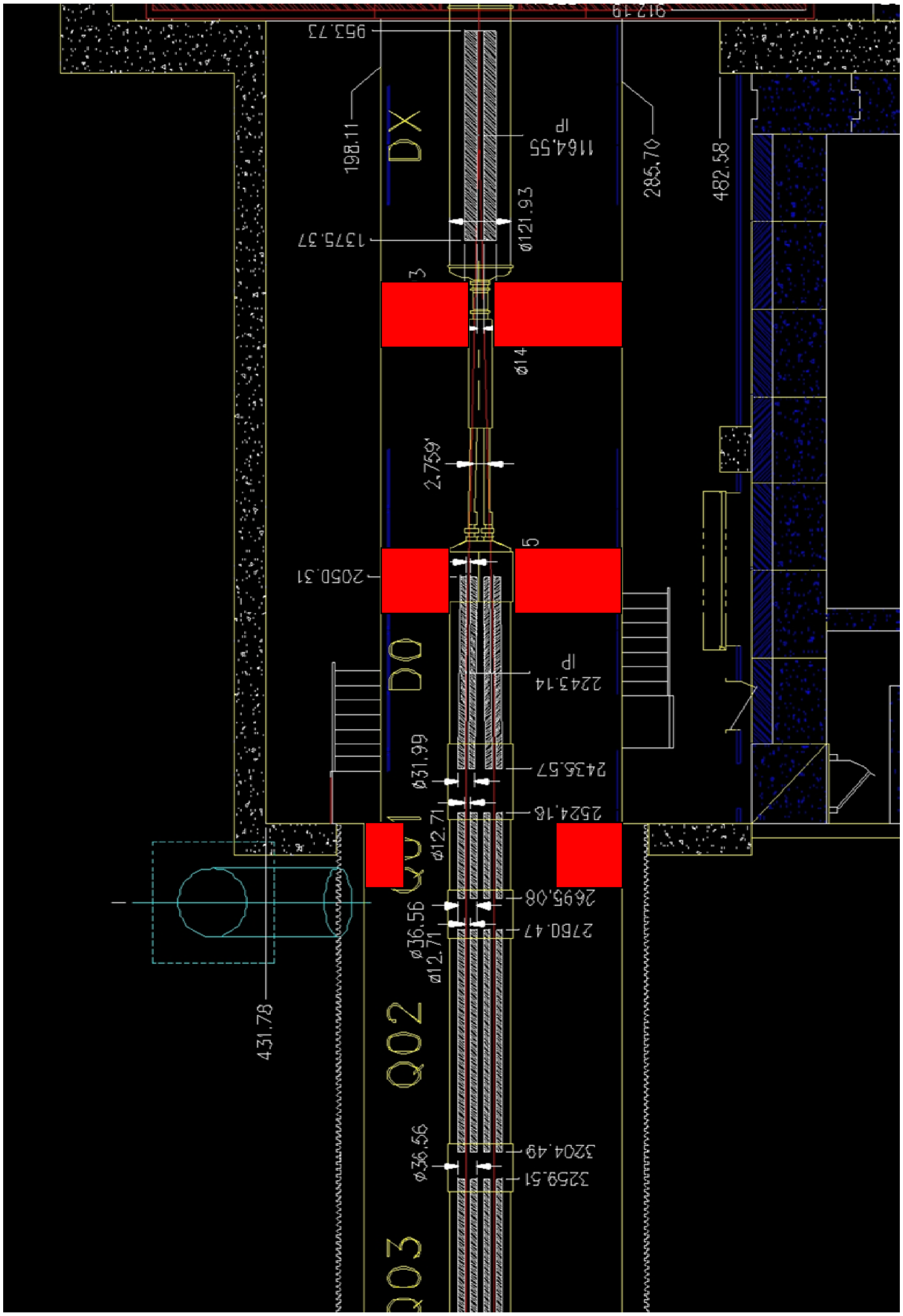

Figure 13. This figure shows a plan view of the South tunnel and the possible locations of three shield walls. Gap-4 of the MuID is just off the top of the page, Q3 is visible at the bottom of the page. Shield walls are shown as red blocks (they will need to have ceilings. Distances are given in cm.

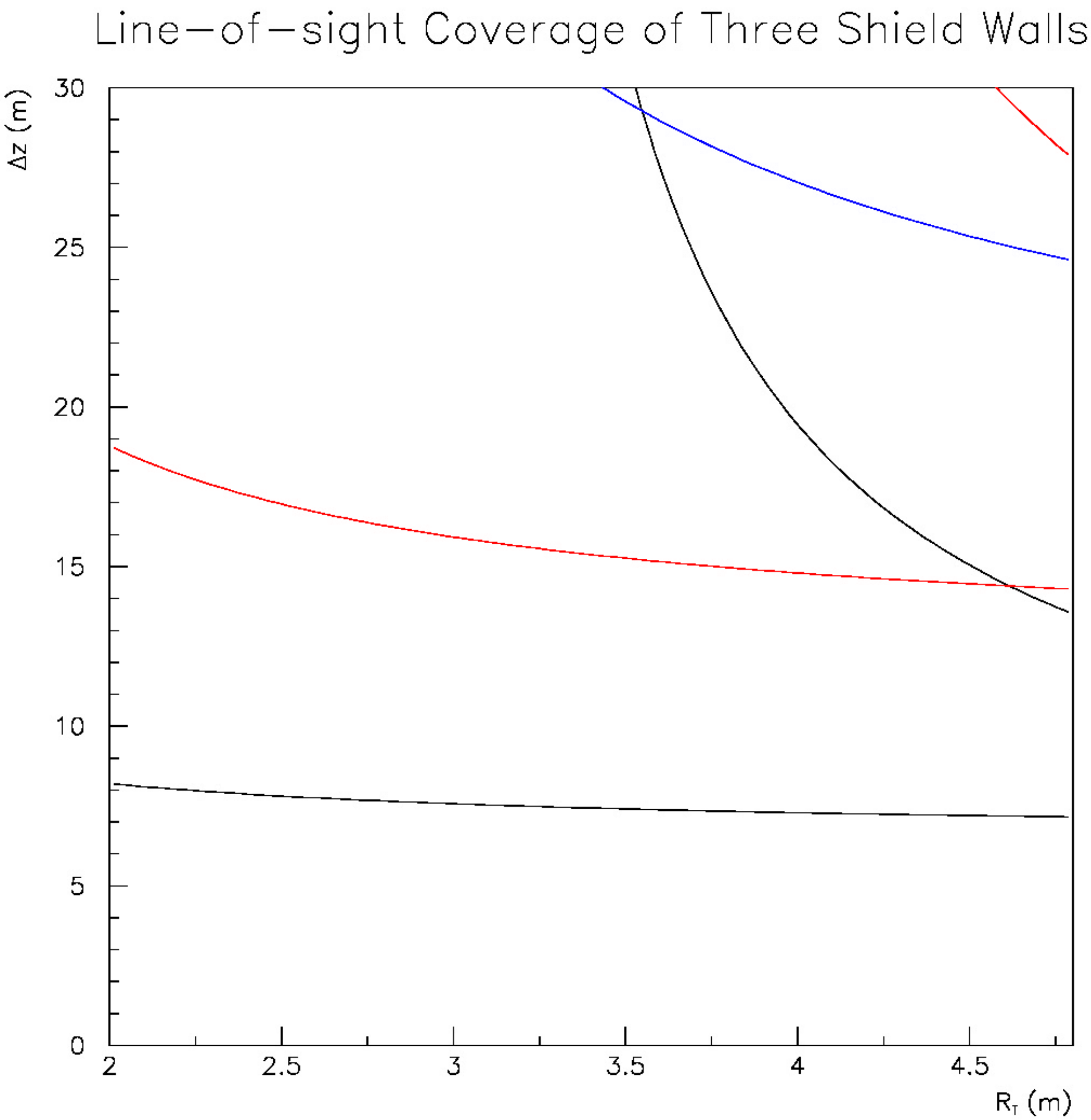

Figure 14. This figure shows the regions of z that the three shield walls of Figure 13 protect as a function of the transverse distance from the beam. Regions within the black lines are covered by the downstream-most wall, those within the red are shielded by the middle wall, and those above the blue line are shielded by the upstream-most wall. This plot is for the inside of the ring which has a larger transverse extent on the mezzanine to support a wall. One can see that there are no holes. The same plot for the outside of the ring has some small holes, which could be plugged by allowing the wall to overhang the mezzanine slightly. For this case the upstream wall appears to be redundant. Note that 8 meters or so immediately upstream of the panels are not shielded. The only way to shield this part of the pipe is with a box surrounding the DX magnet, which is impractical on a number of fronts.